



Oxidative photopolymerization of thiol-terminated polysulfide resins. Application in antibacterial coatings

Abraham Chemtob, N Feillée, Christian Ley, Arnaud Ponche, S Rigolet, C Soraru, Lydie Ploux, D Nouen

► To cite this version:

Abraham Chemtob, N Feillée, Christian Ley, Arnaud Ponche, S Rigolet, et al.. Oxidative photopolymerization of thiol-terminated polysulfide resins. Application in antibacterial coatings. Progress in Organic Coatings, 2018, 121, pp.80-88. 10.1016/j.porgcoat.2018.04.017 . hal-02170484

HAL Id: hal-02170484

<https://hal.science/hal-02170484>

Submitted on 12 Dec 2019

HAL is a multi-disciplinary open access archive for the deposit and dissemination of scientific research documents, whether they are published or not. The documents may come from teaching and research institutions in France or abroad, or from public or private research centers.

L'archive ouverte pluridisciplinaire **HAL**, est destinée au dépôt et à la diffusion de documents scientifiques de niveau recherche, publiés ou non, émanant des établissements d'enseignement et de recherche français ou étrangers, des laboratoires publics ou privés.

Oxidative Photopolymerization of Thiol-Terminated Polysulfide Resins.

Application in Antibacterial Coatings

**Abraham Chemtob,^{*1,2} Noémi Feillée,³ Christian Ley,³ Arnaud Ponche,^{1,2} Séverinne Rigolet,^{1,2}
Charline Soraru,^{1,2} Lydie Ploux,^{1,2} Didier Le Nouen^{2,4}**

¹ Université de Haute-Alsace, CNRS, IS2M UMR7361, F-68100 Mulhouse, France

² Université de Strasbourg, France

³ Université de Haute-Alsace, LPIM EA4567, F-68100 Mulhouse, France

⁴ Université de Haute-Alsace, Université de Strasbourg, CNRS, LIMA UMR7042, F-68100 Mulhouse, France

Abstract

A UV photoinduced cross-linking of non-modified commercial poly(disulfide) resins (Thioplast) is reported via the air oxidative photocoupling of terminal thiol functions. Catalyzed by a photogenerated guanidine base (TBD), this step-growth photopolymerization is useful to maximize disulfide functions content. The mechanism proceeds through thiol deprotonation into thiolate anions, further oxidized into thiyl radicals, eventually dimerizing into disulfide cross-links. Starting with a detailed structural characterization of the thiol-terminated resin, photooxidative kinetics are studied under exposure to a polychromatic medium-pressure Hg arc using Raman and infrared spectroscopy. The effects of irradiance, film thickness, photobase concentration, resin molar mass, and content of an additional polythiol monomer (reactive diluent) have been investigated. In an effort of upscaling, irradiation under a 365 nm LED panel has enabled the fast preparation of 1.5 μm thick cross-linked poly(disulfide) coatings in a matter of minutes. Capitalizing on the ability of residual thiol groups to react with silver cations, a post-functionalization has been successfully performed, leading to films exhibiting at their surface stable thiolate-silver bonds as proved by X-ray photoelectron spectroscopy. Despite the well-established biocide action of silver ions, no antibacterial action has been evidenced by confocal fluorescence microscopy because of insufficient release.

Keywords: UV-curing, polysulfide, sulfur, thiol, antibacterial, photobase generator

^{*} To whom correspondence should be addressed: abraham.chemtob@uha.fr; tel: +33 3 8960 8834

1. Introduction

Discovered as early as in the 1920s, poly(disulfide) (PdS) was the first synthetic rubber to be marketed in the United States [1, 2]. After having initially drawn great attention as a substitute for natural rubber in tires production, this target application was gradually left in favor of more suitable polymers such as polybutadiene and its derivatives [3]. The main obstacles to a large scale utilization of PdS included processability issues, thermal instability and insufficient mechanical properties as regards to compression and abrasion. Nevertheless, PdS elastomer has flourished in niche markets including technical joints for aerospace, construction and double glazing [4]. Four distinctive properties make it particularly attractive for these specific applications: impermeability to water vapor, high resistance to solvents, durability, and low temperature flexibility. Commercial development has been driven by two major achievements: firstly, the development of a preparation method to low-molecular weight liquid PdS oligomers — often referred to as *polysulfide prepolymers* or *Thiokol®* — having internal disulfide bonds, and containing at least two thiol functions: $\text{HS}-(\text{R}-\text{SS})_n-\text{SH}$. The oxidation of SH groups into SS bonds remains today the major reaction pathway to induce cross-linking. Secondly, the development of PdS oligomers based on bis(ethyl)formal ($\text{R} = \text{CH}_2\text{CH}_2\text{OCH}_2\text{OCH}_2\text{CH}_2$) providing optimum properties to the final elastomer (see structure in **Table 1**) [5, 6]. In most cases, the cross-linking requires 2-component formulation in order to separate the oxidizing agent and the prepolymer [7]. In addition, the base-catalyzed oxidation reaction is slow (on average, between 1 h to 24 h), and requires a high concentration of oxidant (4 - 12 wt%) which may impact the final properties [8]. Finally, the applications are limited to structural materials such as seals, and the perspective of developing PdS coatings has been scarcely explored [9]. Yet, a high concentration of SS functions could confer to the final film specific characteristics [10] such as barrier properties, dynamic behavior, increased refractive index and broadened transparency in the infrared region. In addition, residual thiol groups might make feasible a surface post-functionalization through efficient reactions such as thiol-ene, thiol-Michael or thiol-electronically excited carbonyl compounds [11].

UV curing is currently one of the fastest growing technologies for the eco-efficient production of polymer coatings [12]. The process starts from a liquid film based on a one-component formulation including a photoinitiator as well as a mixture of multifunctional oligomers and monomers. Exposure to UV-Vis radiation induces usually a chain-growth polymerization, yielding eventually a thermoset film [13]. The effectiveness of this method relies on a unique combination of features: absence of organic solvent, reaction at room temperature, short cycle times and small-scale production lines. The use of radiation as a stimulus to trigger the polymerization of PdS resin has been rarely reported in the literature [14-16]. In all cases, thiol terminal groups of PdS resins were subjected to chemical modification. In the 1990s, Morton Inter. Corp. (previously known as Thiokol Chemical Corporation) manufactured several acrylate-terminated polysulfide oligomers. However, the change from a step-growth mechanism to a chain-growth one led to a higher cross-linking density, that caused the

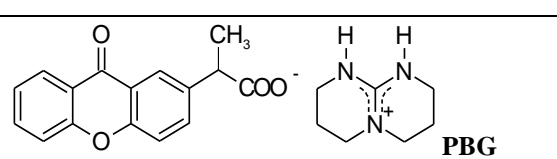
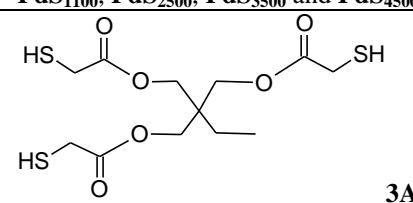
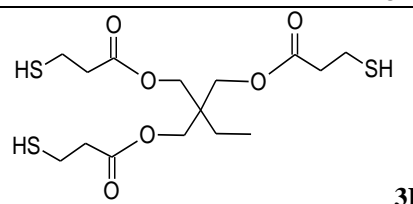
properties of the material to deteriorate substantially [14]. In 2003, several photoactive carbonyl end-groups were introduced by Caddy et al. [15]. Mechanistically, ketone groups reacted from their first triplet state ($^3(n, \pi^*)$ -state) and abstracted hydrogen from additional thiol species (RSH) acting as reducing molecules (co-initiator). A cross-linked disulfide was assumed to form through recombination reactions involving the photogenerated thiyl radicals (RS^\bullet). However, several dozens of hours of UV irradiation were necessary to obtain a solid film. Very recently, Brei et al. introduced terminal alkene groups onto polysulfide resins, thereby enabling them to be photocured via a more efficient radical thiol-ene reaction. Allyl and methallyl-terminated PdS oligomers were synthesized and reacted with polythiol monomers or thiol-terminated PdS oligomers. The resultant solid elastomeric films were tested as adhesives for a target use in aircraft [16]. Good adhesion properties were achieved on various metallic substrates, but only after the incorporation of an organosilane, 3-mercaptopropyltrimethoxysilane, playing the role of adhesion promoter.

We report herein an alternative photoinduced cross-linking process using non-modified commercial thiol-terminated PdS resins (Table 1), and based on the oxidative photocoupling of SH functions into disulfide. In contrast to previous reports, keeping the step-growth polymerization mechanism should maximize the disulfide functions content and allow retention of the excellent properties of poly(disulfide) materials. Radiation control of polymerization relies on the photogeneration of a superbase catalyst (1,5,7-triazabicyclo[4.4.0]dec-5-ene: TBD) through a photobase generator (xanthone propionic acid-protected TBD, **PBG**, see Table 1) [17]. Using this **PBG**, we have recently demonstrated the feasibility of multiple thiol air oxidation of polyfunctional thiol monomers to yield disulfide cross-linked films [18, 19], but the photooxidative polymerization of PdS resin is unprecedented. In terms of mechanism, given that thiols are more acidic than alcohols by an average of about 5 pK_a units ($pK_a = 5-11$), TBD ($pK_a \approx 13.5$) can readily react with a thiol to form a thiolate anions RS^- acting as a much better electron donor [20]. This shift enables oxidation reaction by atmospheric oxygen to form thiyl radicals. Subsequent dimerization of thiyl radicals to disulfide ($RS-SR$) results in cross-linking. Because oxidation is ensured by atmospheric oxygen, the issue of UV attenuation from conventional inorganic oxidizing agents dispersed as particles (MnO_2 , $NaBO_2 \cdot H_2O_2$, $Na_2Cr_2O_7$) is circumvented.

We start with a detailed structural characterization of the PdS resin (Table 1) using liquid ^{13}C and 1H NMR spectroscopy. The kinetics of photooxidative curing for a 1.5 μm -thick PdS-based sample were studied by Raman and infrared spectroscopy under different experimental conditions as regards to irradiance, film thickness, **PBG** concentration, molar mass of PdS resin, and the content of an additional polythiol monomer behaving as reactive diluent (see structure in Table 1). For these optimization experiments, a polychromatic medium-pressure Hg arc ($\lambda > 330$ nm) was employed whose focused radiation enabled only small samples' preparation. In an effort of upscaling, an LED array providing a monochromatic radiation at 365 nm made possible the rapid production (3 min) of

solid cross-linked PdS coatings on large surfaces. The structure of the insoluble photopolymer was examined by ^{13}C solid-state NMR. Capitalizing on the ability of residual thiol groups to react with silver cations, a post-functionalization was performed to form films exhibiting at their surface stable thiolate-silver bonds as proved by X-ray photoelectron spectroscopy (XPS). Assuming the biocide action of silver ions possibly released from the films, their antibacterial properties were assessed in presence of bacterium *Escherichia coli* through confocal fluorescence microscopy.

Table 1. Chemical structures of the compounds used in this study

Type	Structure
Photobase generator	 <p>PBG</p> <p>PdS_x where x is the molecular weight in g mol^{-1} PdS₁₁₀₀, PdS₂₅₀₀, PdS₃₅₀₀ and PdS₄₅₀₀</p>
Polythiol monomer	 <p>3A</p>
	 <p>3P</p>

2. Material and methods

2.1. Materials

2-(9-oxoxanthene-2-yl)propionic acid 1,5,7-triazabicyclo [4.4.0]dec-5-ene salt **PBG** used as photobase generator was purchased from TCI. The four Thioplast® PdS resins were kindly donated by Akzo Nobel. For sake of clarity, they are designated in the rest of the study as **PdS_x**, where x is their average molecular weight given by the manufacturer: **PdS₁₁₀₀** (G4, 1.3 Pa s), **PdS₂₅₀₀** (G20, 10-20 Pa s), **PdS₃₅₀₀** (G1, 41-52 Pa s), **PdS₄₅₀₀** (G10, 38-50 Pa s). The numbers in brackets are their commercial name and viscosity. The trithiol monomers, trimethylolpropane tris(3-mercaptopropionate) (**3A**, 357 g mol^{-1}) and trimethylolpropane tris (3-mercaptopropionate) (**3P**, 399 g mol^{-1}), were obtained from Bruno Bock. Chloroform (> 99 %) was purchased from Sigma-Aldrich. NaCl, AgNO₃, and Luria-Bertani culture medium were purchased from Sigma-Aldrich. Propidium iodide, a fluorescent indicator of bacteria was obtained from Thermo-Fisher. All reagents were used as received without further purification.

2.2. Oxidative photopolymerization of PdS resins

A typical **PdS/PBG** formulation was prepared by dissolving 20 mg of **PBG** in 4 mL of chloroform containing 0.48 g of PdS resin. Photolabile, this homogeneous mixture was then deposited onto a KBr or glass substrate by spin coating (5 s at 1000 rpm and 10 s at 2000 rpm) to obtain a 1.5 μm -thick film, the thickness value was verified by a 3D surface profilometer (Bruker). Irradiation was performed by two devices: a medium-pressure Hg-Xe arc equipped with a 365 nm reflector (Hamamatsu L8251, 200 W) and a filter ($\lambda > 330$ nm) to prevent direct excitation of disulfide functions which may photodissociate SS bonds resulting in the formation of thiyl radicals by a non-oxidative mechanism [19]. During a photopolymerization experiment, the emitted light was directed towards the sample for 900 s by a waveguide placed at 3 cm and perpendicular to the sample. The total irradiance measured at the film surface was 290 mW cm^{-2} ($\lambda = 330 - 550$ nm). The second radiation source is a 365 nm LED panel (Phoseon Technology FJ200) which allowed obtaining a solid film after 180 s of exposure. The irradiance was 560 mW cm^{-2} . This second irradiation system enabled the preparation of larger samples (10×10 cm), making possible the characterization of the polymer formed by techniques requiring a greater amount of material such as solid-state NMR. In all cases, no heat post-treatment was performed.

2.3. Functionalization of cross-linked PdS coatings by silver ions

The polymerized PdS films on silicon wafer were immersed in a AgNO_3 aqueous solution (5 mM) for 30 min. After extensive washing with distilled water, they were then immersed 3 times in a chloroform solution (15 min each time) and sonicated (frequency 45 kHz) in order to sterilize them.

2.4. Characterization techniques

Confocal Raman microscopy enabled the recording of Raman spectra using an in via Raman reflex microscope from Renishaw. The excitation wavelength was provided by a He-Ne laser from Renishaw emitting 17 mW cm^{-2} at 633 nm. The objective used was N PLAN 50 \times Leica with a numerical aperture of 0.75. A 600 l mm^{-1} grating optimized for visible light was used to disperse the light on a CCD NIR deep depletion Peltier cooled detector camera. A 30 s exposure and a 10 spectra accumulation were needed to obtain a reasonable signal-to-noise ratio. The conversion rate of thiol functions was determined by integration of the Raman SH stretching band at 2570 cm^{-1} before and after irradiation. Raman mapping profiles were achieved by displacement of the optical plate holding the sample. A spectrum was taken every micrometer on a $260 \mu\text{m}$ -long line.

Real-time Fourier transform infrared (RT-FTIR) spectra were obtained with a Bruker Vertex 70 spectrophotometer equipped with a liquid nitrogen cooled mercury-cadmium-telluride (MCT) detector working in the rapid scan mode. The resolution of the spectra was 4 cm^{-1} with an average of 4 scans

s⁻¹. The conversion rate of thiol functions over time was determined by integration of the SH stretching band at 2570 cm⁻¹. Transmission FTIR was also used to determine the fraction of insoluble parts in the cross-linked films (gel content). In a typical experiment, a FTIR spectrum of as-synthesized poly(PdS_x) film was initially taken, then the film was immersed in chloroform during 10 min. A new FTIR measurement was then performed after film drying. Immersion-drying cycles were repeated three times. A steady spectrum was considered to indicate a constant film thickness, suggestive of a completely insoluble film.

X-ray photoelectron spectrometry (XPS) analysis was carried out using a Gammatdata Scienta SES 2002 X-ray photoelectron spectrometer under ultra-high vacuum ($P < 10^{-9}$ mbar). The monochromated Al K α source was operated at a current of 30 mA and 14 kV, with a 90° nominal take-off angle (angle between the sample surface and photoemission direction). During acquisition, the pass energy was set to 200 eV for high-resolution spectra. Classical Scofield sensitivity factors were used for peak fitting procedures with CASAXPS software. All line shapes used in peak fitting procedures were a mix of 30 % Gaussian and 70 % Lorentzian shapes.

¹H and ¹³C liquid NMR (400 MHz) spectrum of PdS resins were recorded at room temperature on a Bruker Advance 400 spectrometer equipped with 5 mm Z-gradient QNP (¹H, ¹³C, ¹⁹F, ³¹P) probe for routine spectroscopy. The chemical shifts were referenced to the residual proton signal of the solvents CHCl₃ at 7.26 ppm for ¹H.

Solid-state ¹³C MAS+DEC NMR experiments were performed at room temperature on a Bruker Advance II 400 spectrometer operating at $B_0 = 9.4$ T (Larmor frequency $\nu_0 = 400.17$ MHz). Single pulse experiment was recorded with a double channel 2.5 mm Bruker MAS probe, a spinning frequency of 30 kHz and a $\pi/2$ pulse duration of 2.9 μ s and a 5 s recycling delay. ¹H spin lattice relaxation times (T_1) were measured with the inversion-recovery pulse sequence. Typically, 64 scans were recorded. Chemical shifts reported thereafter are relative to tetramethylsilane ¹H. The deconvolution of the experimental ¹H MAS spectrum was carried out with the DMfit software.

Profilometry measurement of the photopolymerized pattern was carried out using a Dektak 150 (Bruker) profilometer.

Characterization of antibacterial properties. The antibacterial properties of photopolymerized films were evaluated using the bacterium *Escherichia coli* (*E. coli*) SCC1 which produces a green fluorescent protein in normal metabolic conditions [21]. Bacteria (stored in frozen state at -80 °C) were grown overnight at 30 °C on agar plate of lysogeny broth culture medium (LB, Sigma-Aldrich), pre-cultured with a colony in LB liquid medium (18 h at 30 °C), and finally cultured with 10 % of the pre-culture (4 h at 30 °C). Then bacteria were recovered by centrifugation and suspended in an Na⁺Cl⁻ aqueous solution at 9 g L⁻¹ (150 mM, pH = 6.8) [22]. Bacteria suspension was adjusted to achieve an absorbance of 0.01 (5×10^6 bacteria mL⁻¹) at 600 nm. The films on silicon wafer treated with AgNO₃ (T) aqueous solution were immersed in 3 mL of this *E. coli* suspension. They were incubated for 3 h at 30 °C, then rinsed 3 times with NaCl aqueous solution to remove unattached bacteria without creating

an air-surface interface [23]. Clean silicon wafer (**SW**) and non-treated PdS film (**NT**) were also subjected to the same treatment in order to provide standardization of experimental data and comparing the reproduction experiments (internal control). *E. coli* bacteria, potentially damaged by Ag^+ ions released in their culture medium, were stained by addition of 1 μL of propidium iodide, a fluorescent (red) indicator that penetrates bacteria whose wall is made sufficiently porous by silver ions. The films were then observed in the last rinsed solution using a confocal fluorescence microscope in reflection mode (LSM700, Carl Zeiss) equipped with a water immersion lens (focal length of 2 mm). On each film, images were randomly taken in 10 different areas. These images were then processed by ImageJ V.1.49q software to determine the amount of bacteria that adhered to the substrate (green and red bacteria referred to as "living" and "dead" respectively) and among them, those that have been damaged by silver ions ("dead" bacteria). Each experiment was performed on three treated surfaces and three untreated surfaces. The experiment was repeated twice. The significance of differences between average populations on the treated films (**T**; μ_{T}) and the control substrates (**NT** and **SW**; μ_{NT} and μ_{SW}) was given by the Student t-test [36] (hypothesis H_0 : $\mu_{\text{T}} = \mu_{\text{NT}}$ or μ_{SW}).

3. Results and discussion

3.1 Characterization of PdS oligomers and PBG

3.1.1 UV-Vis spectroscopy

The absorption spectra of **PdS**₁₁₀₀ and **PBG** in acetonitrile are given in **Figure 1** (λ : 220 – 600 nm). On the same plot appear also the emission spectra of the medium-pressure Hg-Xe arc used as radiation source. The PdS resin shows a strong absorption band between 230 and 320 nm with a maximum at 248 nm ($\epsilon_{248} > 3.5 \times 10^3 \text{ M}^{-1} \text{ cm}^{-1}$). It is known that the disulfide derivatives have a first absorption band around 250 nm which is characteristic of SS bonds and is related to the π - σ^* molecular orbitals transition [24]. In this UV-C region, nevertheless, we cannot completely neglect a contribution of the thiol chromophore which weakly absorbs at 238 nm [25]. However, its low concentration compared to the SS repeating unit and its weak molar extinction coefficient tends to limit its contribution [25]. The absorption spectrum of the **PBG** shows a maximum at λ_{max} (UV-C) = 242 nm with two shoulders at 262 nm and 289 nm, and a second maximum at λ_{max} (UV-A) = 343 nm. In comparison, TBD (not shown) only absorb weakly at 190-230 nm ($\epsilon_{193\text{nm}} = 3 - 7 \times 10^3 \text{ M}^{-1} \text{ cm}^{-1}$). Therefore, in the studied wavelength range, UV-Vis absorption spectrum of **PBG** is not governed by the TBDH⁺ cation, but the xanthone propionate anion. Accordingly, the absorption spectrum of xanthone is essentially identical to that of **PBG** (not represented).

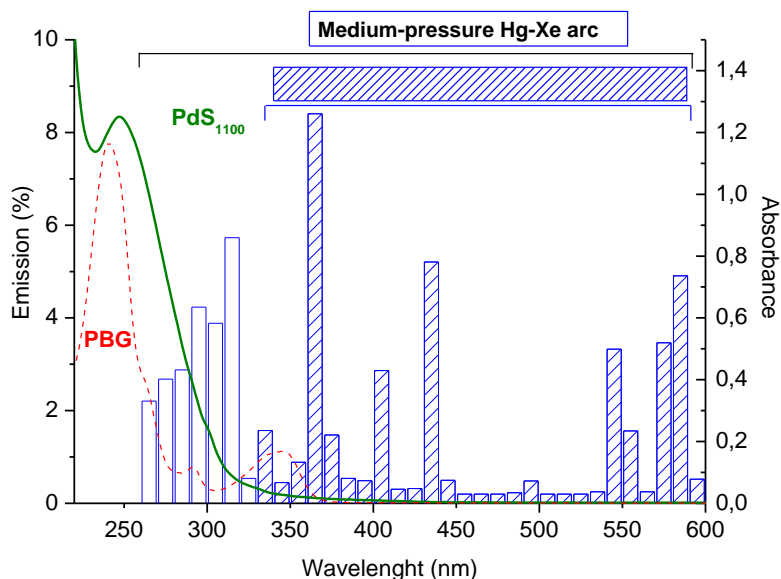


Figure V.1 Absorption spectra of **PdS₁₁₀₀** resin and **PBG** in acetonitrile ($3.4 \cdot 10^{-4}$ M) and emission spectra the Hg-Xe medium pressure arc with and without filter.

3.1.2 NMR spectroscopy

Presumably the chemistry of the formation of PdS oligomer is based on an equilibrating polycondensation reaction between two reactants: a *dihalogenated compound*, bis(2-chloroethyl)formal (Cl-R-Cl, R = CH₂CH₂OCH₂OCH₂CH₂) and *alkali sodium polysulfide* (Na₂S_x where $x = 2 - 5$). The ¹³C NMR spectrum of **PdS₁₁₀₀**, shown in **Figure 2A**, displays 5 major resonances in agreement with this mechanism. Firstly, the 3 intense carbon signals of the polyether chain (*D*, *E* and *F*) arise at 95.4, 66.1 and 38.8 ppm. Additionally, the characteristic methylene carbon in α position of the terminal thiol group (*B*) is visible at 24.5 ppm. The neighboring oxygen-adjacent carbon (*C*) appears at 69.7 ppm. It is shifted downfield (+ 3 ppm) compared to carbon *E* because the sulfur atom is more shielding in the thiol state than in the disulfide state. These assignments are in agreement with the idealized thiol-functionalized poly(disulfide ether) structure shown in the insert of Figure 2A [26, 27]. However, the PdS resin does not seem pure owing to the two resonances at 32.2 and 67.5 ppm indicating the presence of monosulfide species (identified by the letter M in the spectrum). In addition, other low intense peaks (marked with a star) are visible in the spectra, suggesting that other impurities are present in the starting material, probably trisulfide derivatives and hydrolyzed halogenated compounds. However, the precise assignment of these weak resonances is out the scope of this manuscript. According to the manufacturer, **PdS₁₁₀₀** was prepared with 2 mol% of 1,2,3-trichloropropane to obtain a trifunctional resin. However, the ¹³C NMR study testifies the absence of any tertiary carbon, whose resonance would be expected at 49.9 ppm. This hypothesis was also supported by DEPT ¹³C NMR experiment (not given) [28, 29]. This result suggests that the trifunctional cross-linking agent was probably hydrolyzed. Therefore, **PdS₁₁₀₀** will be considered as a difunctional resin in the rest of this study.

The ^1H NMR spectra of **PdS₁₁₀₀** is shown in **Figure 2B**. The signal from the thiol proton appears as a triplet (*a*, 1.57 ppm) as it is split by the two neighboring methylene protons (*b*). In turn, these sulfur adjacent methylene protons (*b*, 2.72 ppm) appear as a quartet after their signal is split by both the thiol proton (*a*) and the oxygen-adjacent methylene protons (*c*, 3.61 ppm). In the repeating disulfide unit, proton *f* is adjacent to SS bonds. Split by the sulfur-adjacent methylene protons (*e*, 3.80 ppm), proton *f* (2.89 ppm) appears as triplet. As expected, the central methylene protons (*d*, 4.71 ppm) surrounded by two oxygen atoms appear as singlet. In addition, two resonances indicate the presence of monosulfide compounds (6 % of total protons) at 3.71 and 2.80 ppm. The resonances in the 3.5-3.7 ppm region at and 1.75 ppm (water) confirm the existence of impurities. In addition, the number-average molecular weight (M_n) was determined by ^1H NMR spectroscopy. To calculate the number of repeating units in the PdS₁₁₀₀ chain, the peak areas of the well resolved -OCH₂O- singlet (*d*) and -SH triplet (end-group, *a*) were obtained. The experimental M_n value of 991 g/mol was relatively consistent with the value provided by the provider (1100 g/mol).

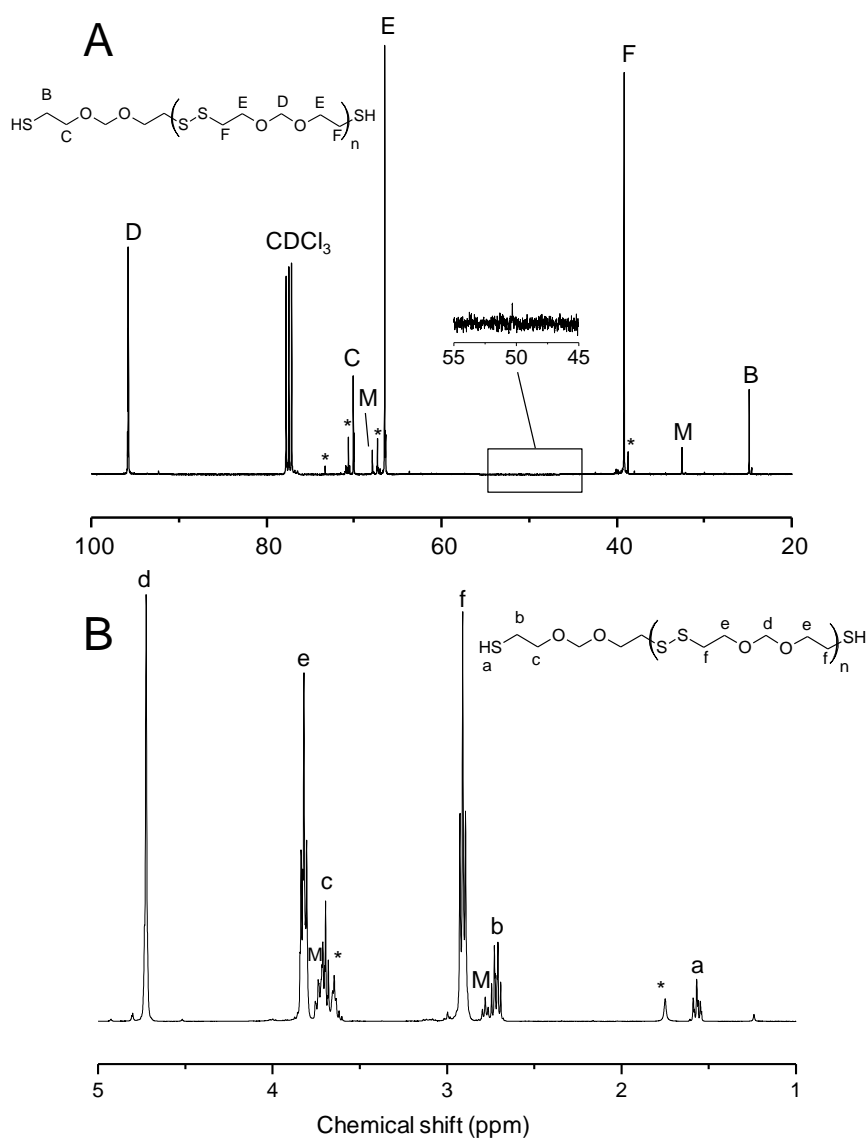


Figure 2. ^{13}C (A) and ^1H (B) NMR spectra of **PdS₁₁₀₀** resin in CDCl_3 , M: monosulfide derivatives and *: impurities.

3.2 Kinetics of PdS oxidative photopolymerization

3.2.1 FTIR and Raman spectroscopy

A 1.5 μm -thick **PdS₁₁₀₀** film (including 4 wt% **PBG** with respect to the resin) was irradiated for 15 min under a filtered medium-pressure Hg arc ($\lambda = 330 - 600 \text{ nm}$, 290 mW cm^{-2}). A dry transparent film insoluble in a range of conventional organic solvents (THF, toluene, ethanol) was obtained. Interestingly, the insolubility of the film cannot be attributed to the cross-linked structure since **PdS₁₁₀₀** is a difunctional resin, but rather to the intrinsic hydrophobicity of the poly(disulfide) backbone. FTIR and Raman spectra before and after irradiation are given in **Figure 3**. The decay of the vibrational band $\nu_{\text{S-H}}$ at 2560 cm^{-1} (FTIR) and 2565 cm^{-1} (Raman) were both relatively consistent, both showing a thiol consumption of 70 % (FTIR) and 80 % (Raman). The decrease of the stretching band $\nu_{\text{C-SH}}$ at 666 cm^{-1} gave a similar conversion value. Due to their symmetry, disulfide bond signals are inherently weak in IR and not detectable. By contrast, the $\nu_{\text{C-SS}}$ (648 cm^{-1}) and $\nu_{\text{S-S}}$ (507 cm^{-1}) modes were clearly visible in the Raman spectrum before irradiation. Surprisingly, their intensity was not affected by photopolymerization. Presumably, the formation of new disulfide bonds by thiol oxidation only account for a 10 % increase, which may be not sufficient to induce a significant modification of the Raman spectrum.

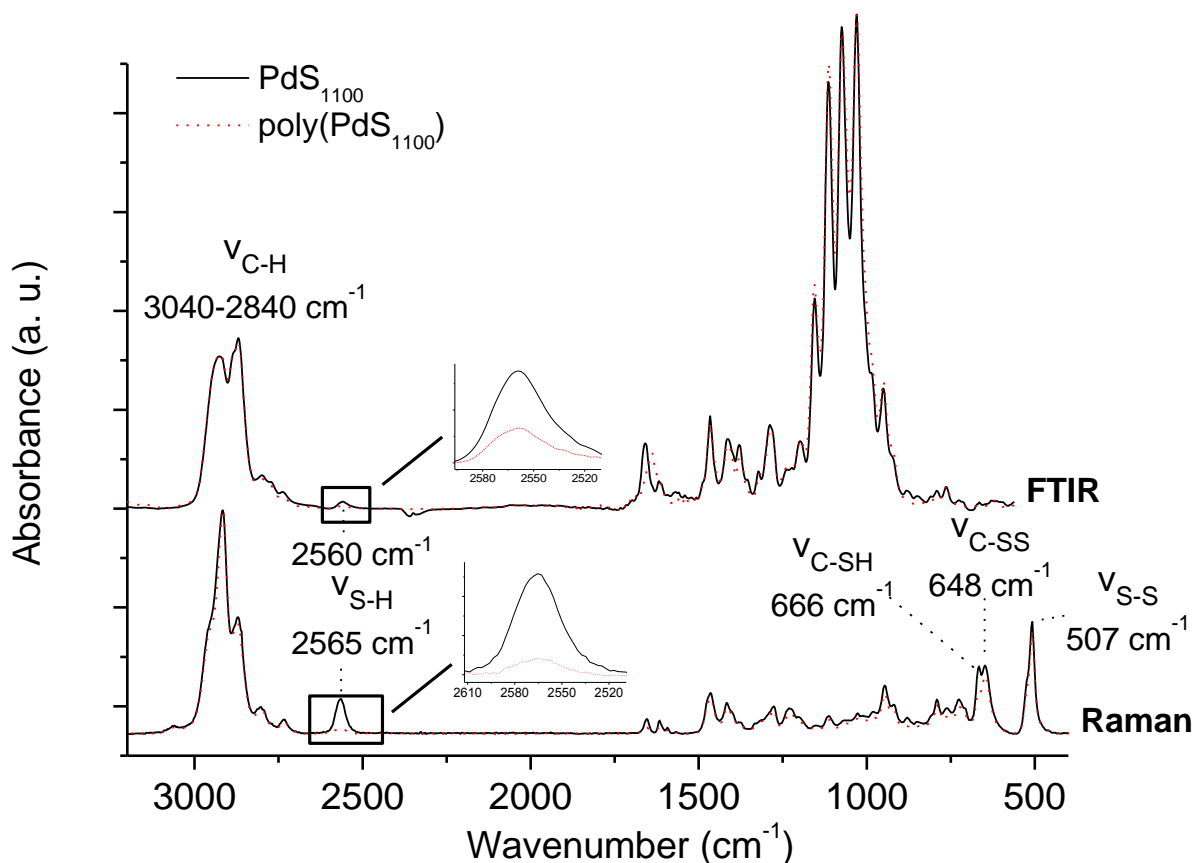


Figure 3. FTIR and Raman spectra of **PdS₁₁₀₀/PBG** film before (solid line) and after 15 min of irradiation (dash line) under medium-pressure Hg arc ($\lambda > 330$ nm).

3.2.2 Influence of various experimental parameters

Real-time FTIR spectroscopy has been implemented to extract thiol conversion *versus* irradiation times. The kinetics data were obtained by monitoring the decrease of the $\nu_{\text{S-H}}$ band at 2560 cm^{-1} throughout irradiation. **Table 2** gives the conversion after 15 min irradiation depending on film thickness ($1.1 - 11.1\text{ }\mu\text{m}$) and irradiance ($0 - 290\text{ mW cm}^{-2}$).

The release of TBD plays a major role as no reaction was observed without irradiation (run **1**). The conversion was found to be the greatest at maximum irradiance (run **6**, 290 mW cm^{-2} , 79 %) and at the lowest thickness (run **7**, $1.1\text{ }\mu\text{m}$, 86 %). A steady fall in final conversion was observed when the irradiance (runs **1-6**) or the film thickness (run **7 - 12**) was gradually decreased. The strong effect of film thickness on reaction kinetics suggests an oxygen diffusion-controlled regime. As proved in previous studies [19], atmospheric oxygen plays a crucial role in the mechanism of thiol oxidation. Accordingly, strong inhibition was observed under a nitrogen atmosphere, reducing the final thiol conversion to 20 % (**Figure 4A**). **Figure 4B** displays the results of thiol conversion as a function of irradiation time upon varying **PBG** concentration from 2 wt% (35 %) to 8 wt% (100 %). A strong impact of **PBG** content was demonstrated until a threshold value of approx. 6 wt%. An additional control experiment confirmed that direct irradiation of **PdS₁₁₀₀** film without **PBG** did not cause any polymerization.

Table 2. Influence of film thickness and irradiance on thiol conversion during the irradiation of a **PdS₁₁₀₀/PBG** film (filtered Hg-Xe arc, 15 min irradiation).

Run	Irradiance mW cm^{-2}	Thickness μm	Thiol conversion %
1	0	1.5	0
2	53		40
3	106		58
4	156		62
5	220		65
6	290		79
7	290	1.1	86
8		2.2	70
9		3.4	59
10		5.1	47
11		6.3	40
12		11.1	25

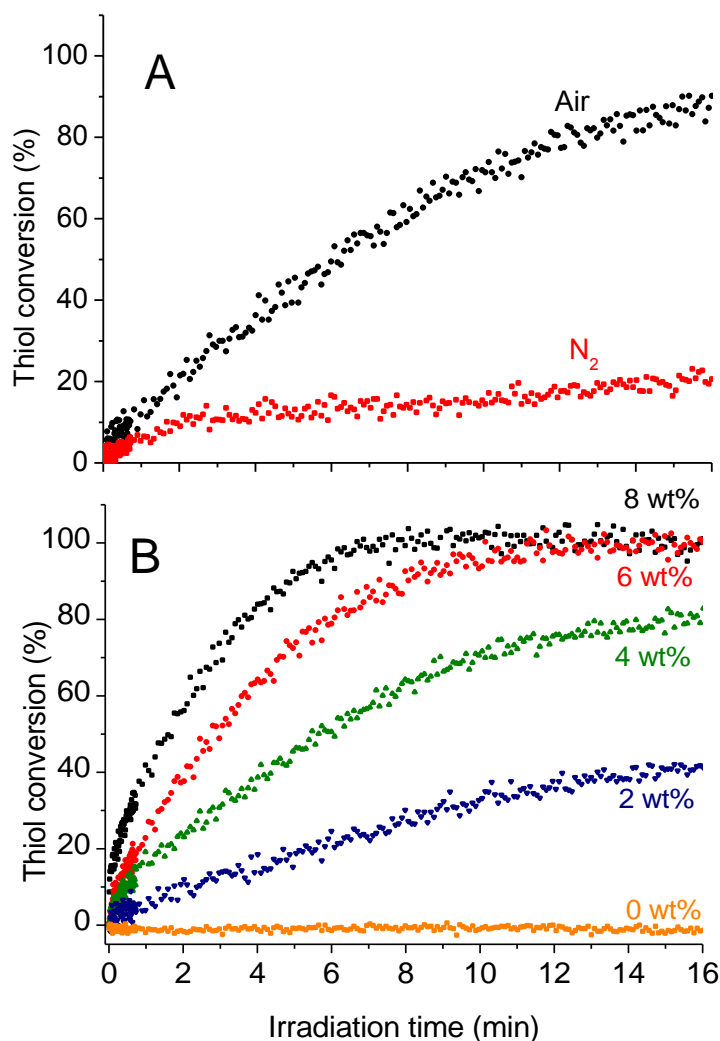


Figure 4. Conversion-times curve obtained by RT-FTIR for **PdS₁₁₀₀/PBG** film (thickness: 1.5 μm) when exposed to filtered medium-pressure Hg arc ($\lambda = 330 - 600 \text{ nm}$, 290 mW cm^{-2}). Plot **A** shows the effect of atmosphere composition for a sample containing 4 wt% **PBG**. Plot **B** illustrates the influence of PBG concentration (0 – 8 wt%) under air.

Figure 5A shows the effect of the molar mass of the difunctional prepolymers (1100 - 4500 g mol^{-1}) on the conversion kinetics. In all experiments, film thickness (1.5 μm) and **PBG** content (4 wt%) were kept constant. One must note that dry films were obtained regardless of the resin molecular-weight. As expected, the intensity of the vibrational $\nu_{\text{S-H}}$ mode at 2560 cm^{-1} decreases upon using higher molecular weight oligomers due to a lower concentration of SH functions. This causes a higher signal-to-noise ratio, and consequently, the precise evaluation of the $\nu_{\text{S-H}}$ band area has become more difficult for the highest molecular-weight resins. Despite the underlying uncertainties, the overall trend is that the conversion rates were hardly affected by the change in molecular weight. This result may seem surprising when considering that the **PBG**/SH molar ratio is four times higher in **PdS₄₅₀₀** system than for **PdS₁₁₀₀**. This effect is likely to be offset by two negative effects of molecular weight on reaction

kinetics. A higher molar mass resin implies a viscosity increase (see experimental section for viscosity data) which can decrease both the mobility of the polymer chains and the permeation of atmospheric oxygen.

To generate a three dimensional network, oligomer **PdS₁₁₀₀** was copolymerized with a trithiol monomer, exhibiting either an acetate (**3A**) or propionate structure (**3P**), and acting as reactive diluents (see structures in Table 1). The reaction kinetics of **PdS₁₁₀₀**/Monomer film (62/38 %wt ratio) were monitored by RT-FTIR spectroscopy (Figure 5B). The trimercaptoacetate **3A** did not slow down the initial reaction rate. However, a limiting conversion of 60 % was reached compared to 80 % when **PdS₁₁₀₀** was homopolymerized. Physical termination may be responsible for the lower final conversion when switching from a linear polymer to a network structure. Network growth is stopped due to diffusional limitation preventing the coupling reaction between thiyl terminated chain-ends. Upon replacing **3A** by **3P**, both initial reactivity and final conversion declined, and a plateau of conversion at 44 % was reached after 10 min irradiation. This difference is probably due to the lower reactivity of mercaptopropionate derivatives compared to their acetate homologues.

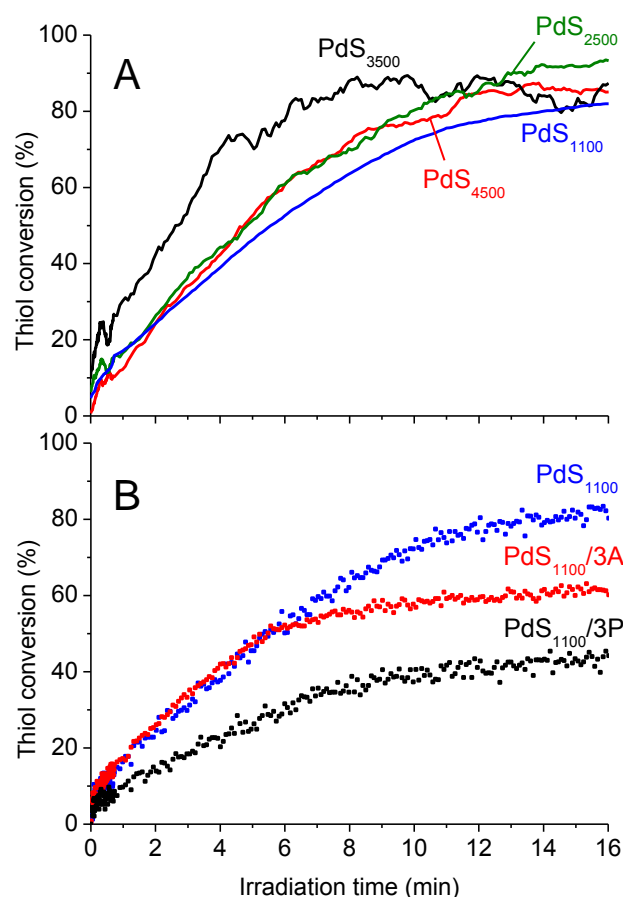


Figure 5. A. Influence of **PdS_x** molecular weight ($x = 1100$ to 4500 g mol⁻¹) on photopolymerization kinetics. **B.** Effect of acetate (**3A**) or propionate (**3P**) reactive diluent (38 wt%) on **PdS₁₁₀₀** (62 wt%) photopolymerization. Thiol conversion is an overall thiol conversion from monomer and resin. In all experiments, thickness was maintained at $1.5\ \mu\text{m}$ and the concentration of **PBG** 4 wt% with respect to active materials (monomer and resin). Irradiation was provided by a filtered medium-pressure Hg-Xe arc.

3.3 Production of poly(disulfide) coatings under 365 nm LED

The use of a LED array emitting at 365 nm (560 mW cm^{-2}) is appropriate because of the **PBG**'s significant absorption at this specific wavelength (see Figure 1). The photopolymerization kinetics obtained by analyzing the specimen sample every min by FTIR revealed that only 3 min irradiation were necessary to achieve almost full conversion (97 %). Although the luminous efficiency of LEDs is not dramatically higher compared to conventional lamps, the narrower band emission allows optimization of the fraction of emitted light absorbed by the photocatalyst. In addition, the narrow band of LED often circumvents interactions with other UV absorbing species such as PdS resin (Figure 1).

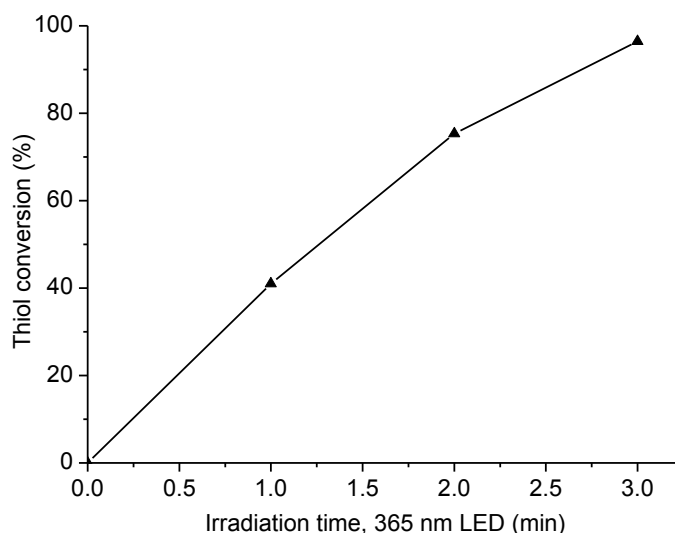


Figure 6. Thiol conversion kinetics during the irradiation of **PdS₁₁₀₀/PBG** by a 365 nm LED.

The ^{13}C NMR spectra of the **PdS₁₁₀₀** oligomer and the poly(**PdS₁₁₀₀**) after irradiation are compared side-by-side in **Figure 7**. The polymerized sample being insoluble, a solid-state NMR analysis was performed using MAS+DEC technique. Few changes in chemical shift distinguished the oligomer and polymer spectra. Narrow resonances were obtained suggesting a mobile and homogeneous polymer structure. The thiol-adjacent carbons *B* (24.5 ppm) and *C* (29.5 ppm) almost disappeared, agreeing with a quantitative conversion of SH into SS bonds (> 96 %) as supported by FTIR data. The oxygen-adjacent carbons (*E* and *D*) as well as the disulfide-adjacent carbon (*F*) moved slightly upfield after photopolymerization because of the difference of environment between an analysis in liquid and solid-state condition.

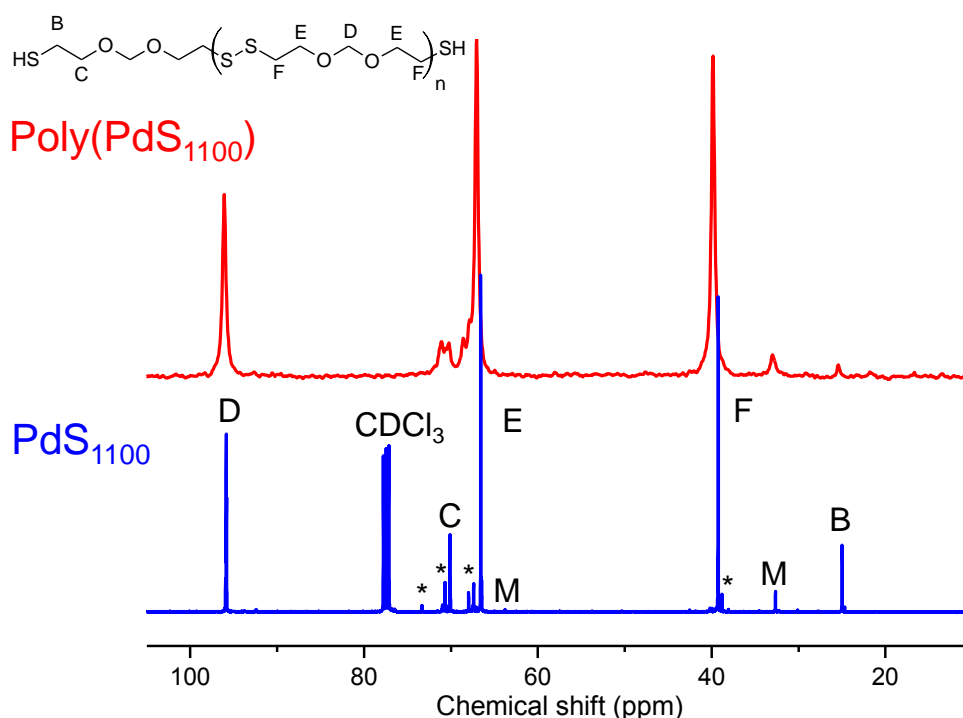
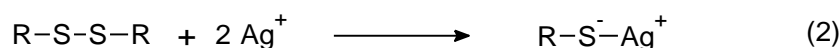
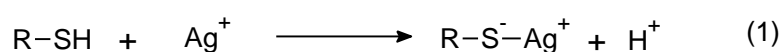


Figure 7. ^{13}C liquid NMR spectrum of PdS_{1100} in CDCl_3 (bottom) and MAS+DEC RMN of $\text{poly}(\text{PdS}_{1100})$ after 3 min irradiation with a 365 nm LED (top).

3.4 Application in antibacterial coating

3.4.1 Surface functionalization of $\text{poly}(\text{PdS}_{1100})$ with AgNO_3 aqueous solution

Ag^+ is recognized as an efficient bactericidal species having a broad spectrum of activity [30]. In recent years, the use of silver cations as a biocide in solution, but also in suspension as silver nanoparticles, has expanded [31]. While metallic silver is biologically inert, ionization occurs in the presence of humidity or in contact with body fluids. Biologically active Ag^+ ions are thus released although the precise mechanism has remained elusive. For the design of antibacterial polymer coatings, the main stream method relies on the incorporation of silver nanoparticles by making nanocomposite polymer material containing antibacterial agent reservoirs [32]. In addition to the challenge of synthesizing silver nanoparticles and ensuring their dispersion into a polymer matrix, the activity against bacteria also depends on numerous factors such as nanoparticles' release rate, and their ability to be oxidized in situ. We attempted to develop an alternative strategy to antibacterial coatings without synthetic nanoparticles based on surface modification of PdS films by ionic silver solution. The surface then constitutes a direct reservoir of silver ions which could be ideally released in the liquid medium containing the bacteria. Functionalization is driven by the ability of residual thiol or even disulfide bonds to react towards silver ions by oxidative addition (eq. 1-2).



The ability to modify polymerized **PdS₁₁₀₀** surface was examined. Films showing various thiol conversions (30, 60 and 100 %) were prepared through 365 nm LED irradiation by varying the exposure times. Subsequently, they were immersed in an aqueous solution of silver nitrate (5 mM) for 30 min. XPS surface analysis of the three treated PdS films as well as a non-treated specimen (100 % conv.) was carried out. **Figure 8** shows the S2p_{3/2, 1/2} spectra since the carbon, nitrogen and oxygen spectra showed minimal variation. Deconvolution of the spectra showed the characteristic two spin-orbit pairs (S2p_{3/2} and _{1/2}) at 163.6 and 164.8 eV accounting for the sulfur atoms present as thiol or disulfide. Further oxidized sulfur species such as sulfonate gave a distinctive contribution at binding energy of 166 eV or higher, which accounts for less than 3 % of sulfur atoms at the surface. As expected, samples with an incomplete thiol conversion had a higher tendency to be over-oxidized by atmospheric oxygen during film storage [33]. Interestingly, only treated samples showed a distinctive peak at 161.2 eV related to S-Ag thiolate bonds. This result supports the selective functionalization of films, which represents up to 9 % of the superficial S atoms for the sample displaying at the beginning 60 % converted thiol. The molar proportion of the three groups of sulfur species (disulfide/SH, over-oxidized S, and S-Ag) was detailed in **Table 3**. A larger fraction of grafted silver ions was observed when thiol conversion was incomplete, confirming the covalent grafting of Ag⁺ ions on a thiolate species and the higher affinity of thiol for silver ions compared to disulfide [34]. However, a non-negligible amount of silver (1.3 %) was even observed in the case of the fully converted film. This low value can be understood on the basis that silver ions can dissociate disulfide bonds to form stable thiolate-silver bonds [35].

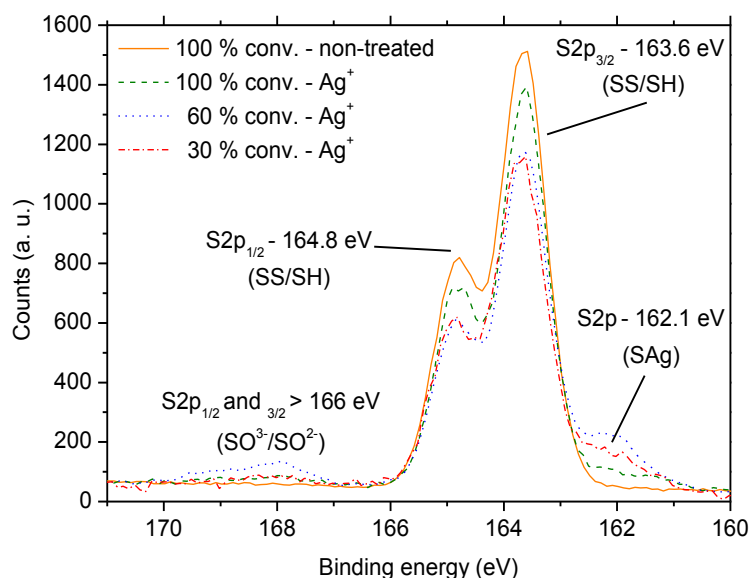


Figure 8. S_{2p} XPS spectra of poly(**PdS₁₁₀₀**) displaying various thiol conversions (100, 60 and 30 %) after immersion in an aqueous AgNO₃ solution (5 mM) for 30 min. For comparison, a non-treated sample is also shown (solid line).

Table 3. Atomic percentage of silver and proportion of the three different sulfur species obtained by deconvolution of the XPS spectra S_{2p} . The poly(**PdS**₁₁₀₀) films varying in thiol conversion (30, 60 and 100 %) were prepared by photopolymerization and post-functionalization with a solution of AgNO₃ (5 mM, 30 min).

Thiol conversion (mol%)	Amount of silver in the film (mol%)	SS / SH (%)		Over-oxidized S (%)		S-Ag (%)	
		S2p _{3/2}	S2p _{1/2}	S2p _{3/2}	S2p _{1/2}	S2p _{3/2}	S2p _{1/2}
100%	1.3	45.49	44.53	0.72	0.71	4.32	4.23
60%	4	38.76	37.94	2.54	2.49	9.24	9.04
30 %	3	40.97	40.10	1.46	1.43	8.11	7.94

3.4.2 Assessment of antibacterial properties

The antibacterial properties of treated poly(**PdS**₁₁₀₀) films (60 % conv.) (called **T**) were evaluated with the bacterium *E. coli*. They were compared to the performances of clean substrates (bare silicon wafer, **SW**) and non-treated poly(**PdS**₁₁₀₀) coatings (**NT**). The results in **Figure 9** show average and standard deviation of the surface colonization by “living” and “dead” bacteria. In the case of “living” bacteria on PdS surfaces (**T** or **NT**) and **SW**, the probability analysis indicates that the disulfide coatings whether treated or non-treated are slightly favorable to bacterial adhesion. Conversely, **T** and **NT** PdS surfaces are statistically not colonized differently. So there is no anti-bacterial effect due to the presence of silver ions on the surface. With regard to the population of dead bacteria, the probability analysis clearly indicates that the number of bacteria on the three different systems must be regarded as similar ($\mu_T = \mu_{NT} = \mu_{SW}$). Therefore, bacteria have not been degraded significantly, leading to the conclusion that treated PdS films lack of antibacterial properties.

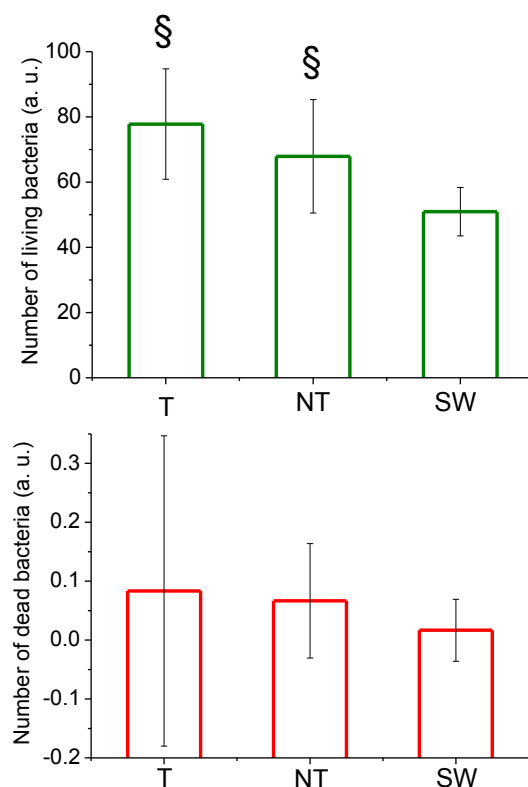


Figure 9. Mean and standard deviation of the colonization of "living" and "dead" bacteria. § symbol indicates significant differences to **NT** and **SW** samples respectively (p -value < 0.05)

This outcome may seem surprising because similarly treated self-assembled monolayers (SAMs) containing only a maximum silver content of 2.5 % turned out to be antibacterial [37]. No proven bacterial activity was obtained in our case despite a relatively high amount of silver (4 mol% in the first 10-nanometer layer the film probed by XPS, see Table 3). To understand this result, a calculation taking into account only the volume of the top 10 nm demonstrates that the maximum molar concentration of silver theoretically released into the medium is approx. 10^{-7} M. By contrast, the threshold inhibitory Ag^+ concentration on *E. coli* SCC1 (NaCl 9 g L^{-1}) was estimated around 10^{-5} and 10^{-6} M (unpublished data), which is also congruent with results reported in the literature for *E. coli* [38]. Therefore, the first hypothesis is to consider that too few silver ions are present in the environment because of an insufficient concentration of S-Ag functions within the film. Increasing this concentration remains challenging because thiols are end-groups of the PdS oligomer chains. In addition, this maximum concentration of Ag^+ released into the bacterial culture medium may be underestimated by our calculation because only the superficial layer of the coating (10 nm) was taken into account. However, this seems to be a reasonable assumption because only this thickness range can be probed XPS; in addition, the film is cross-linked and subjected to a short functionalization stage (30 min) which may limit the entrapment of Ag^+ within the micrometric film. To account for the lack of activity, another plausible explanation is the high stability of the S-Ag bond which may prevent the release of Ag^+ in the medium. This second hypothesis is the most likely considering that the energy binding of the S-Ag binding is 6 times larger than that of silver chelated by carboxylate groups [39]. To be fully validated, a determination of the Ag^+ concentration released in the aqueous environment is necessary.

4. Conclusions

We have demonstrated oxidative photopolymerization can be applied to the cross-linking of liquid PdS resins. Within minutes, a dry film is obtained under various radiation sources (medium-pressure Hg arc and LED emitting at 365 nm). In addition, the possibility of applying this method to a set of non-modified PdS resins of variable molecular-weight as well as mixtures including polythiol monomers was proved. These results are important to establish thiol-thiol step-growth photopolymerization as a UV curing technology because it paves the way to a control of chemical composition, network structure, and final properties. For the preparation of antibacterial coating, post-functionalization with Ag^+ was performed and supported by XPS analysis. However, the high stability of S-Ag bond may hinder the release of silver ions, thereby preventing the degradation of bacteria. Despite the absence of antibacterial properties, the treated poly(disulfide) film can behave alternatively

as a reservoir of silver ions releasable on demand by, for example, through a suitable ion exchange reaction [40].

5. References

- [1] J.C. Patrick, Mnookin N.M., Br. Patent 302270, 1927.
- [2] J.C. Patrick, Mnookin, N. M., Method of making plastic substances and product obtained thereby, U.S. Patent 1,996,486, 1935.
- [3] H. Lucke, Aliphatic polysulfides : ALIPS, Huthig & Wepf, 1994.
- [4] T.C.P. Lee, Properties and Applications of Elastomeric Polysulfides, Rapra Technology, 1999.
- [5] J.C. Patrick, Polysulphide plastic and process of making, in, Thiokol Corp, U.S. Patent 2,195,380, 1940.
- [6] J.C. Patrick, Preparation of mercaptans, in, Thiokol Corp, U.S. Patent 2,479,542, 1949.
- [7] D. Vietti, M. Scherrer, Polymers Containing Sulfur, Polysulfides, in: Kirk-Othmer Encyclopedia of Chemical Technology, John Wiley & Sons, 2000.
- [8] G.B. Lowe, The cure chemistry of polysulfides, Int. J. Adhes. Adhes., 17 (1997) 345-348.
- [9] Y.N. Khakimullin, Y.N. Minkin, T.R. Deberdeev, G.E. Zaikov, Polysulfide Oligomer Sealants: Synthesis, Properties and Applications, CRC Press, Boca Raton, USA, 2015.
- [10] E.-K. Bang, M. Lista, G. Sforazzini, N. Sakai, S. Matile, Poly(disulfide)s, Chem. Sci., 3 (2012) 1752-1763.
- [11] C. Lowe, C. Bowman, Thiol-X Chemistries in Polymer and Materials Science, Royal Society of Chemistry, 2013.
- [12] R. Schwalm, UV Coatings: Basics, Recent Developments and New Applications, Elsevier Science, 2006.
- [13] J.G. Drobny, Radiation Technology for Polymers, CRC Press, 2010.
- [14] C. Hughes, Synthesising, Characterising and Formulating Acrylated Liquid Polysulfide, in: Morton Report, 1997.
- [15] M. Caddy, T.J. Kemp, Photoactive liquid polysulfides: preparation, characterisation, photocuring and potential applications, Eur. Polym. J., 39 (2003) 461-487.
- [16] M.R. Brei, B.R. Donovan, D.L. Patton, R.F. Storey, Synthesis and thiol-ene photopolymerization of (meth)allyl-terminated polysulfides, J. Appl. Polym. Sci., 134 (2017) 45523..
- [17] A. K., R. Endo, Application to photoreactive materials of photochemical generation of superbases with high efficiency based on photodecarboxylation reactions, Chem. Mater., 22 (2013) 4461-4463.
- [18] N. Feillée, A. Chemtob, C. Ley, C. Croutxé-Barghorn, X. Allonas, A. Ponche, D. Le Nouen, H. Majjad, L. Jacomine, Photoinduced Cross-Linking of Dynamic Poly(disulfide) Films via Thiol Oxidative Coupling, Macromol. Rapid Commun., 37 (2016) 155-160.
- [19] N. Feillée, M. De Fina, A. Ponche, C. Vaulot, S. Rigolet, L. Jacomine, H. Majjad, C. Ley, A. Chemtob, Step-growth thiol-thiol photopolymerization as radiation curing technology, J. Polym. Sci. Part A: Polym. Chem., 55 (2017) 117-128.

- [20] E. Rosenthal-Kim, J. Puskas, Green Polymer Chemistry: Investigating the Mechanism of Radical Ring-Opening Redox Polymerization (R3P) of 3,6-Dioxa-1,8-octanedithiol (DODT), *Molecules*, 20 (2015) 6504.
- [21] H. Miao, S. Ratnasingam, C.S. Pu, M.M. Desai, C.C. Sze, Dual fluorescence system for flow cytometric analysis of *Escherichia coli* transcriptional response in multi-species context, *J. Microbio. Meth.*, 76 (2009) 109-119.
- [22] O. Vidal, R. Longin, C. Prigent-Combaret, C. Dorel, M. Hooreman, P. Lejeune, Isolation of an *Escherichia coli* K-12 Mutant Strain Able To Form Biofilms on Inert Surfaces: Involvement of a New *ompR* Allele That Increases Curli Expression, *J. Bacteriol*, 180 (1998) 2442-2449.
- [23] K. Anselme, P. Davidson, A. Popa, M. Giazzon, M. Liley, L. Ploux, Response to comment on "The interaction of cells and bacteria with surfaces structures at the nanoscale", *Acta Biomater.*, 7 (2011) 1936-1937.
- [24] G. Bergson, G. Claeson, L. Schotte, Ultraviolet Absorption Spectra of Saturated Disulphides and, *Acta Chem. Scand*, 16 (1962) 7.
- [25] A.R. Knight, Photochemistry of thiols, in: *The Thiol Group*, John Wiley & Sons, 1974, pp. 455-479.
- [26] A. Mahon, T.J. Kemp, R.J. Coates, Thermal and photodegradation of polysulfide pre-polymers: products and pathways, *Polym. Degradation Stability*, 62 (1998) 15-24.
- [27] A. Mahon, T.J. Kemp, R.J. Coates, Thermal and photodegradation of MnO₂-, NaBO₃- and organic hydroperoxide-cured polysulfides: products and pathways, *Polym. Degradation Stability*, 62 (1998) 187-198.
- [28] W. Mazurek, A.G. Moritz, Carbon-13 NMR of polysulfide prepolymers, *Macromolecules*, 24 (1991) 3261-3265.
- [29] T. Matsui, Y. Miwa, Detection of a new crosslinking and properties of liquid polysulfide polymer, *J. Appl. Polym. Sci.*, 71 (1999) 59-66.
- [30] S. Silver, L.T. Phung, G. Silver, Silver as biocides in burn and wound dressings and bacterial resistance to silver compounds, *J. Ind. Microbio. Biotech.*, 33 (2006) 627-634.
- [31] M. Rai, A. Yadav, A. Gade, Silver nanoparticles as a new generation of antimicrobials, *Biotechno. Adv.*, 27 (2009) 76-83.
- [32] A. Travan, E. Marsich, I. Donati, S. Paoletti, Silver Nanocomposites and Their Biomedical Applications, in: *Nanotechnologies for the Life Sciences*, Wiley-VCH, 2007.
- [33] D.G. Castner, K. Hinds, D.W. Grainger, X-ray Photoelectron Spectroscopy Sulfur 2p Study of Organic Thiol and Disulfide Binding Interactions with Gold Surfaces, *Langmuir*, 12 (1996) 5083-5086.
- [34] B. Xu, G. Gonella, B.G. DeLacy, H.-L. Dai, Adsorption of Anionic Thiols on Silver Nanoparticles, *J. Phys. Chem. C*, 119 (2015) 5454-5461.

- [35] R.G. Nuzzo, D.L. Allara, Adsorption of bifunctional organic disulfides on gold surfaces, *J. Am. Chem. Soc.*, 105 (1983) 4481-4483.
- [36] B. Scherrer, *Biostatistiques*, Chenelière Education, 2007.
- [37] J. Amalric, P.H. Mutin, G. Guerrero, A. Ponche, A. Sotto, J.-P. Lavigne, Phosphonate monolayers functionalized by silver thiolate species as antibacterial nanocoatings on titanium and stainless steel, *J. Mater. Chem.*, 19 (2009) 141-149.
- [38] G. Mulley, A. Tobias, A. Jenkins, N. R. Waterfield, Inactivation of the Antibacterial and Cytotoxic Properties of Silver Ions by Biologically Relevant Compounds, *PLoS ONE* 9 (2014) e94409.
- [39] R.A. Bell, J.R. Kramer, Structural chemistry and geochemistry of silver-sulfur compounds: Critical review, *Environ. Toxicol. Chem.*, 18 (1999) 9-22.
- [40] A.H. Pakiari, Z. Jamshidi, Nature and Strength of M–S Bonds (M = Au, Ag, and Cu) in Binary Alloy Gold Clusters, *J. Phys. chem. A*, 114 (2010) 9212-9221.